CHEM-E8135 Microfluidics and BioMEMS

Scientific Posters
3.3.2021

Ville Jokinen and Sami Franssila

Scientific poster

- A standard way of communicating science at a conference to peers. An alternative to an oral talk.
- A ”typical” mid-sized/large conference, e.g.: 5 plenary talks (all conference attendants see these), 50 talks in parallel sessions (split into 2-5 simultaneous parallel sessions based on topics), **200 posters.**
- A poster presentation is a combination of: **1.** the poster itself and **2.** the researcher being present at the poster at specified time to introduce the poster and discuss its content. The presentation sometimes includes a short, 1 or 2 minutes, prepared talk given to the entire conference.
- The poster has to work both **1.** supporting your presentation but also **2.** as a standalone.

Poster hall from µTAS2018, the main microfluidics conference, in Kaohsiung, Taiwan

Poster project

The poster project is worth 30 points.

The project is done in pairs (or individually)

The grading is based on a grading rubric with 6 different categories. 2 categories relating to research done for poster, 2 for the graphical design and 2 for the presentation at the poster.

Only the final version of the poster is graded.

For posters done as pairs, the points for presentation are individual, both for the poster itself both get the same points.

There will be a mandatory short chat with the teachers about the poster midway of the project **14.3** between 11-12.

7.4 is the poster session. It will be done in Zoom. We divide the 2h session equally for all posters. Each poster is first presented and then discussed.

Poster evaluation practice:

Today, we look at several example posters and practice using the **graphical part** of the rubric, and you can see how your assessments compare to the teachers.

Since evaluating posters is *partly subjective*, you will get to know the preferences of the teachers who do the grading.

You can practice along. You can find the rubric in MyCourses and you will be given some time to evaluate the poster before the teachers start their discussion.

Use the rubric given to grade the 7 posters.
30s per poster.

Top 2 criteria: **(12 total)**
Research, we cant grade them today.

Middle 2: **(10 total)**
Graphical layout
Mark them like that, using the letter assigned for the poster, all 7 posters into the same rubric.

Bottom 2: **(8 total)**
Presentation, capability to discuss the topic, How well poster works with presentation/discussion.
We cant grade these today.

	0	1	2	3	4	5
Content **4 points**		There are at least 2 papers included that fit the poster topic.		The papers that are chosen are well chosen and their combination gives a good overview of the topic.		The poster is the students own original fusion of the chosen papers that gives an excellent and interesting overview of the topic.
Depth **8 points**		The poster is very superficial, no significant results are presented and the matter is poorly connected to the topics learned on course. There are some clear errors.		The poster goes to some depth on the topic OR nicely utilizes the principles learned on the course. There are clear results on the poster. No or only minor errors.		The topic is handled in a level suitable for masters students and utilizes the principles learned on the course. The poster presents several well chosen results. No or only minor errors.
Structure **5 points**		The structure of the poster is confusing and makes the content more difficult to understand. A quick glance of the poster does not illuminate the topic beyond reading the title.		Structure of the poster is by-the-book, one topic follows another. It does not confuse the visitor but neither does the structure offer assistance in understanding the topic. A quick glance on the poster gives an understanding of the topic		The structure of the poster guides the visitor to understand the conclusions, results and their relations to each other. A quick glance on the poster gives the visitor an understanding of the poster topic and an overview of the content.
Effort **5 points**		The poster looks like it was done with minimum effort and looks unfinished and unappealing.		The poster shows that decent effort has went into the poster and as a result the poster looks good.		The student has clearly put in great effort and polish to make the poster look appealing and professional.
Presentation **4 point**		The intro presentation is either too casual and brief or too unfocused and long. The poster works poorly with the presentation, pictures are e.g. too small, key information is in wrong place (e.g. bottom corner).		The intro presentation is of suitable length (on this course, 1 minute) and gives a good starting point for discussion. The poster works decently with the presentation. Some topics could have been placed more centrally.		The presentation is of suitable length, easy to follow and informative on the topic and content of the poster. The poster works seamlessly with the presentation.
Capability to discuss the topic **4 points**		The student can only discuss the topic by answering basic questions.		The student can very nicely answer most questions about the topic at hand, but can only give rudimentary own thoughts about the topic.		The student can discuss the topic with the visitors at a level of a nice scientific conversation, which includes the students own thoughts as well.

A
C
B
B
C
A

A

MOTIVATION

- The intriguing intrinsic photoluminescence (PL) of gold nanoparticles (AuNPs) has received increasing attention over the last years due to potential applicability in a great number of biosensing, imaging or optical labelling applications [1,2].
- The nonbleaching nature of their PL signal, strongly correlated with plasmon resonances and size, enables their probing by fluorescence spectroscopy techniques, such as fluorescence correlation spectroscopy (FCS) toward label-free sensing applications.
- Despite several available reports, the field of PL - based biosensing applications using FCS, remains partially unexplored, due to incomplete elucidation of the mechanism behind PL.

GOALS

- Investigate the PL and diffusion behavior of AuNPs of spherical/rod-like shape and different sizes, in solution, by performing one-photon excited FCS assays under excitation at 405 nm (interband transition of gold).
- Extract the diffusion parameters by fitting the obtained PL autocorrelation curves.
- Correlate the hydrodynamic diameter of the AuNPs obtained using Stokes-Einstein equation with results obtained from transmission electron microscopy (TEM) and dynamic light scattering (DLS).

SAMPLES AND INSTRUMENTATION

A. Gold nanospheres (AuNSs) stabilized with cetyltrimethylammonium chloride (CTAC)
B. Gold nanorods (AuNRs) stabilized with cetyltrimethylammonium bromide (CTAB)

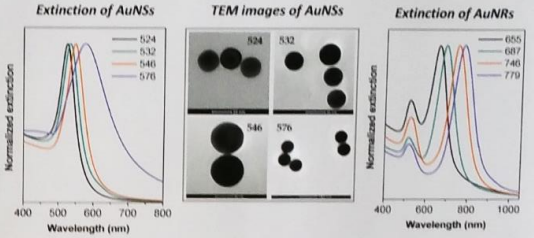

FCS measurements:

- MicroTime200 confocal fluorescence system equipped with Olympus IX71 microscope
- Pulsed excitation provided by **405 nm laser diode** (40 MHz, 40 μW)
- Two SPAD detectors for cross-correlation analysis
- 60×/1.2=NA objective, 430LP emission filter and 150 μm pinhole
- ***Fluorescence Lifetime Correlation Spectroscopy (FLCS) analysis***

DLS measurements:

- Zetasizer Nano ZS90 instrument (Malvern Instruments) equipped with a He-Ne laser (633 nm, 5 mW).

Gold nanospheres

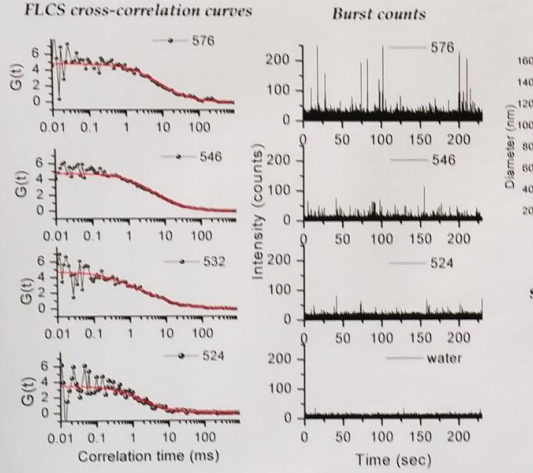

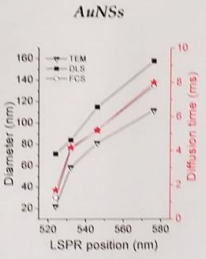

Stokes Einstein Equation

$$d_{FCS} = \frac{kT}{3\pi\eta TD}$$

d_{FCS} = hydrodynamic diameter
k = Boltzmann constant
T = temperature
η = solvent viscosity
D = diffusion coefficient

Gold nanorods

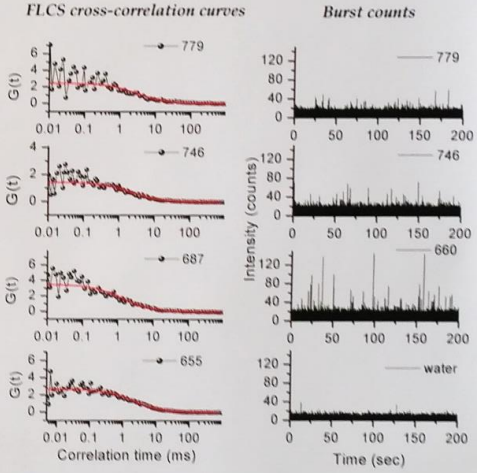

Sample	$\langle \tau_d \rangle$* (ms)	$\langle D \rangle$** (μm²/sec)	$\langle d_{FCS} \rangle$ (nm)	$\langle d_{TEM} \rangle$ (nm)	$\langle d_{DLS} \rangle$ (nm)
AuNSs 524 CTAC	1.7	16	30.4	22	71
AuNSs 532 CTAC	4.2	6.4	76	58.7	84
AuNSs 546 CTAC	5.4	5.2	93.6	81.5	115
AuNSs 576 CTAC	8	3.6	135.2	112	158

* diffusion time; ** diffusion coefficient

Sample	$\langle \tau_d \rangle$ (ms)	$\langle D \rangle$ (μm²/sec)	$\langle d_{FCS-echic} \rangle$ (nm)	$\langle d_{DLS} \rangle$ (nm)
AuNRs 655	2.2	12.4	39.2	51
AuNRs 687	1.4	20	24.3	33
AuNRs 746	2.3	11.8	41.2	54
AuNRs 779	3.2	8.5	57.3	68

* diffusion time; ** diffusion coefficient

GENERAL CONCLUSIONS

- *Spherical and rod-shaped AuNPs exhibiting intrinsic PL at 405 nm excitation were successfully characterized by FLCS in water solution*
- *The diffusion parameters extracted from cross-correlation analysis using FLCS filters are well strongly related to the size of the diffusing AuNPs.*
- *Hydrodynamic diameters obtained from FCS were compared with values obtained by TEM and DLS*
- *The results obtained here make us confident that by combining the PL properties of AuNPs with the highly sensitive FCS method, reliable label-free sensitive detection methods can be developed.*

B

INTRODUCTION

Three-dimensional (3D) cell culture is an emerging practice in various applications such as drug discovery, disease modelling and stem cell research. Traditional 2D cell culture models are lacking normal interactions between the cells and extracellular matrix (ECM). As a consequence, several problems may occur. For example, pre-clinical drug discovery studies with 2D cultured cells can result in biased results and improper conclusions, which may lead to expensive failures at the later stages of the drug development. 3D culturing of the cells results in more natural growth and improved functionality as 3D culturing resembles *in vivo* micro-environment better. Hydrogels are most common way to culture cells in 3D. Nanofibrillar cellulose (NFC) hydrogel (GrowDex®) has been successfully used in 3D culture of different cell types.

GrowDex is wood-based NFC hydrogel developed for 3D cell culture **(Fig 1.)**. It is biocompatible with human cells and tissues but as a plant based product it does not contain any animal or human derived material. GrowDex efficiently supports 3D cell growth by physically resembling extracellular matrix ECM (1,2,3). The structure and mechanical properties of GrowDex can be tuned to fulfill the requirements of different cell types and it allows the diffusion of nutrients and oxygen.

Under stress GrowDex has shear thinning properties, which make it a pipettable ready-to-use hydrogel.

Figure 1. GrowDex hydrogel.

One of most interesting properties of GrowDex is the **possibility to degrade the hydrogel by cellulase enzyme treatment**, while retaining the grown 3D cell structure. This is important in applications where the grown 3D cell structures are utilized and analyzed in various downstream processes, such as detailed imaging of 3D cell surface (4).

To deepen our knowledge about NFC hydrogel degradation process, a real-time analysis method was developed to observe the degradation kinetics. Various cellulase enzymes were used in concentration series. Additionally, the effect of cellulase enzymes on cell viability was studied *in vitro* with two cell lines.

AIMS OF THE STUDY

1. Develop and optimize a **real-time assay for the analysis of enzymatic degradation** of nanofibrillar cellulose hydrogel
2. Study the degradation **with various cellulase enzymes**
3. Test the **effect of enzyme treatment on cells *in vitro***

MATERIALS AND METHODS

Materials

- GrowDex® hydrogel (UPM, Finland)
- Purified cellulase enzyme mixture (UPM), and cellulase enzymes from *Aspergillus niger*, *Trichoderma viride, and Trichoderma Reesei* (Sigma-Aldrich)
- HepG2 and WA07 cells with culturing medium and supplements

Analysis methods

Nephelometry analysis

Enzymatic degradation of nanocellulose hydrogel was detected with nephelometry technique that measures light scattering in real time (Nepheloskan Ascent, Labsystems, Finland). GrowDex was diluted to 0.7% with PBS. Different enzyme concentrations were prepared by diluting enzyme stock solutions to desired concentrations with PBS (0–500 µg/mg cellulose with UPM enzyme and 0-200 U/ml with Sigma enzymes), respectively. Degradation studies were performed in 96-well format: 100µL of the hydrogel was transferred to 96-well plate (Brandplates pureGrade, Brand GMBH, Germany) and 100µL of cellulase enzyme was added on top of the hydrogel. Immediately after adding the enzyme, the plate was sealed with transparent adhesive film (ThermalSeal RT, Sigma-Aldrich) to prevent evaporation, and the experiment was carried out at 37°C. GrowDex degradation with different enzyme treatments was measured over 24h without shaking and with 60 RPM shaking, respectively.

Determination of glucose

Cellulase enzymes degrade cellulose to glucose mono units. Determination of glucose from degraded GrowDex samples by 3,5-dinitrosalisylic acid (DNS) –assay (5) was performed as a secondary assay after the nephelometry experiments. DNS reacts with reducing sugars, and it is reduced to to 3-amino,5-nitrosalisylic acid, which can be quantified by spectrophotometry. Samples and glucose standard solutions (100µL) were mixed with DNS reagent (150µL) and placed into boiling water for 5 min. The reaction was stopped by placing the samples on ice, 100µL was transferred into 96-well plate (Brandplates pureGrade), and absorbance was measured at 540nm with spectro-photometer (iEMS Reader MF, Thermo Electron Corporation, Finland).

***In vitro* cell cultures**

The effect of the cellulase enzymes on cell viability was examined in vitro **2D cell cultures** with two different cell lines, **HepG2** (HB-8065™, ATCC, VA, USA) and **WA07** (Wicell, WI, USA). For cell viability and growth study, HepG2 cells were seeded in 200 µL on 96-well plate (Nunclon Sphera™, ThermoFisher Scientific). WA07 cells were seeded on Matrigel –coated 96-well plate. After 24 h incubation at 37°C in 5% CO_2, different enzyme concentrations in culture medium were administered to the cells and incubated at 37°C for 24h. **AlamarBlue assay** (ThermoFisher Scientific) was performed prior to and after the enzyme treatment to study the effect of enzyme on the mitochondrial metabolic activity of the cells. Additionally, the effect of cellulase enzyme to **3D cell cultures** in GrowDex was analyzed. HepG2 cells were cultured 3D in 0.8% GrowDex by seeding 600 cells/µl in 100µl hydrogel to Ultra-low attachment 96 well plate (Corning Costar®) and adding 100µl of supplemented culture medium on top. AlamarBlue assay was performed prior to, and after the enzyme treatment. **Live/Dead assay** was performed using calcein-AM for live cells and ethidium homodimer-1 for dead cells.

RESULTS

A clear concentration-dependent kinetics was observed with UPM cellulase enzyme and with cellulase from *Trichoderma Viride* in nephelometric real-time analysis of GrowDex degradation *(Fig 2A and B)*. The light scattering from cellulose nanofibers decreases as the fibers are degraded to soluble sugar molecules. On the contrary, cellulase from *Aspergillus Niger* did not show similar degradation profile (Fig 2C). The result is likely due to different enzymes present in the enzyme products. The shaking of plate during the experiment did not have effect on the degradation speed (data not shown). It was observed that *Trichoderma Viride*, and especially *Aspergillus Niger* enzymes contain glucose, which induced a bias in glucose determination analysis (Fig 2B and C). UPM enzyme does not contain glucose, and degradation resulted in equal glucose amounts with enzyme concentration 100mg/g and above (Fig 2A), suggesting full degradation of cellulose nanofibers.

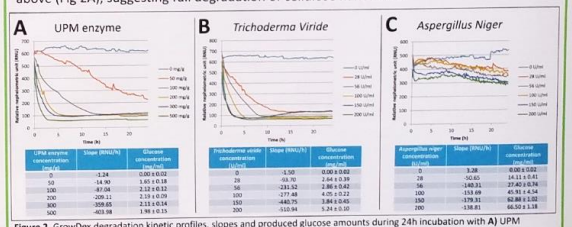

UPM enzyme concentration (mg/g)	Slope (RNU/h)	Glucose concentration (mg/mL)
0	-1.24	0.00 ± 0.02
50	-14.90	1.65 ± 0.18
100	-87.04	2.12 ± 0.13
200	-209.11	2.19 ± 0.09
300	-359.65	2.13 ± 0.14
500	-403.98	1.98 ± 0.15

Trichoderma viride (U/mL)	Slope (RNU/h)	Glucose concentration (mg/mL)
0	-1.50	0.00 ± 0.02
28	-53.70	2.64 ± 0.39
56	-231.52	2.86 ± 0.42
100	-277.48	4.05 ± 0.22
150	-440.75	3.84 ± 0.45
200	-510.94	5.24 ± 0.10

Aspergillus niger concentration (U/mL)	Slope (RNU/h)	Glucose concentration (mg/mL)
0	3.28	0.00 ± 0.02
28	-50.65	14.11 ± 0.41
56	-140.31	27.40 ± 0.74
100	-153.69	45.91 ± 4.54
150	-179.31	62.86 ± 1.02
200	-138.81	66.50 ± 1.18

Figure 2. GrowDex degradation kinetic profiles, slopes and produced glucose amounts during 24h incubation with **A)** UPM cellulase enzyme **B)** Cellulase from *Trichoderma Viride* and **C)** Cellulase from *Aspergillus Niger.*

The effect of UPM cellulase (Fig. 3A) and *Trichoderma Reesei* cellulase (Fig. 3B) on cell viability was examined *in vitro* 2D cell cultures of HepG2 and WA07. It was observed that both cells tolerate 24h enzyme treatments well. The mitochondrial activity was not significantly changed when different enzyme concentration were tested. Slight decrease in viability was seen when highest enzyme concentration were used. This may be related to decreased culture medium content during the incubation with enzyme. HepG2 spheroids cultured 3D in GrowDex showed also good viability after enzymatic removal of GrowDex (Fig. 4). Only few dead cells were observed with Live/Dead staining after 24h incubation with high enzyme concentration (500mg/g), and also AlamarBlue analysis showed good tolerance for cellulase treatment.

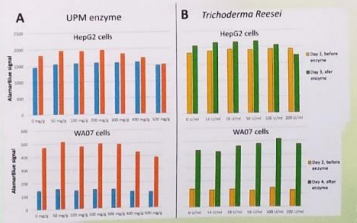

Figure 3. Mitochondrial activity of HepG2 and WA07 2D cultured cells after 24h treament with **A)** UPM cellulase and **B)** *Trichoderma Reesei* cellulase enzymes.

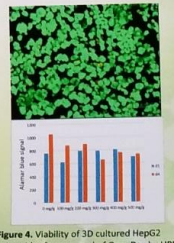

Figure 4. Viability of 3D cultured HepG2 spheroids after removal of GrowDex by UPM cellulase treatment analyzed by **A)** Live/Dead staining (500mg/g), and **B)** AlamarBlue assay

DISCUSSION AND CONCLUSIONS

Degradation of 3D culturing matrix is beneficial in various applications. As human cells do not contain cellulose, cellulase enzyme can be used to remove GrowDex hydrogel without harming the cells. Light-scattering method is convenient method for real-time analysis of cellulose fiber degradation kinetics. Commercial cellulase products contain different amounts of cellulase enzymes such as endoglucanase and β-glucosidase, and impurities that may have an affect on the degradation process.

C

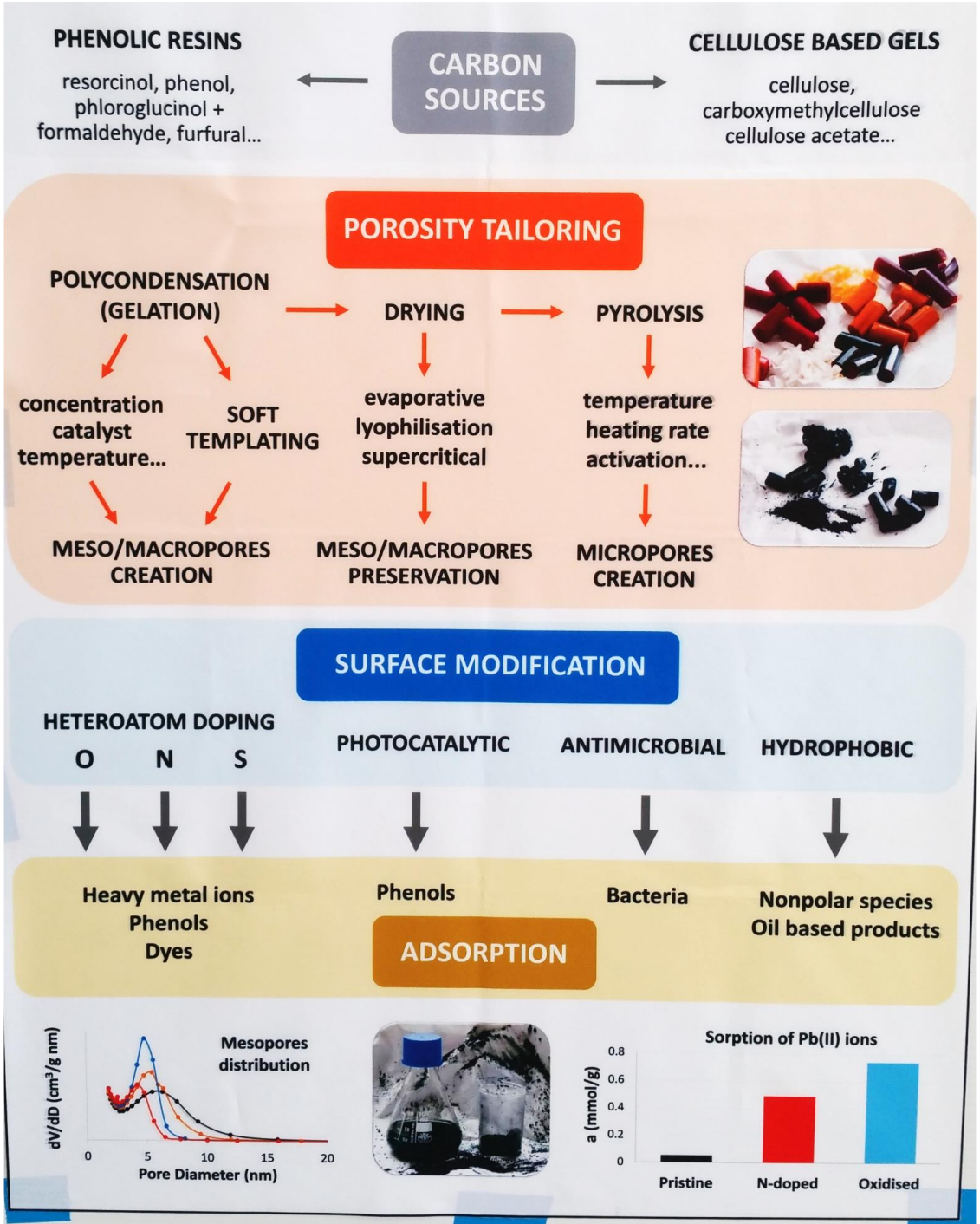
PHENOLIC RESINS
resorcinol, phenol, phloroglucinol + formaldehyde, furfural...
CARBON SOURCES
CELLULOSE BASED GELS
cellulose, carboxymethylcellulose cellulose acetate...
POROSITY TAILORING
POLYCONDENSATION (GELATION)
DRYING
PYROLYSIS
concentration catalyst temperature...
SOFT Ttemplating
evaporative lyophilisation supercritical
temperature heating rate activation...
MESO/MACROPORES CREATION
MESO/MACROPORES PRESERVATION
MICROPORES CREATION
SURFACE MODIFICATION
HETEROATOM DOPING
O N S
PHOTOCATALYTIC
ANTIMICROBIAL
HYDROPHOBIC
Heavy metal ions
Phenols
Dyes
Phenols
ADSORPTION
Bacteria
Nonpolar species
Oil based products
Mesopores distribution
dV/dD (cm³/g nm)
Pore Diameter (nm)
Sorption of Pb(II) ions
a (mmol/g)
Pristine
N-doped
Oxidised

D

form conformal and ultra-thin polymer film, we fabricated hybrid organic-inorganic polymeric film by Molecular layer deposition (MLD). s technique is sequential, self-limiting surface reaction to form conformal and ultra-thin polymer film and uses bifunctional precursors for stepwise uential surface reaction. Also, in comparison with solution-based technique, because MLD is vapor-phase deposition based on ALD, it allows taxial growth of molecular layer on substrate and is especially good for surface reaction or coating of nanostructures such as nanopore, noparticle and nanowire. In this study, organic-inorganic alucone polymeric films were fabricated through coupling reactions between nethylaluminum (TMA) and one of two diols with different carbon-carbon bond order as inorganic and organic precursors, respectively, by olecular layer deposition based on sequential and self-limiting surface reactions. Depending on bond type of organic precursors, such as 1,4-tanediol (BDO) and 2-Butyne-1,4-diol (BYDO), affected their molecular flexibility and showed different aspects in the characterization result.

Introduction

Molecular Layer Assembly

Solution-Based Method

Spin coating | Spraying | SAM

These solution based-approaches have many factors to consider ich as polarity, pH, degradation, and environment concerns, sulting in randomly oriented molecules in amorphous organic films.

Gas-Based Method

CVD | PECVD | ALD

For improving the performance of organic films, it is essential to ntroduce gas-phase approaches, however, it is difficult to precisely control the film thickness and composition at the nanoscale.

C. Molecular Layer Deposition

Molecular Layer Deposition (MLD) is powerful technique for *fabricating conformal ultra-thin organic films with controlled composition and thickness at the molecular level*. This process is based on self-saturating reactions between precursors and the substrate surface. Also it allows epitaxial growth on substrate and is good for surface reaction or coating of nanostructure.

Experiment

Molecular Layer Deposition

A. Experimental Set-Up

All **hybrid organic-inorganic alucone MLD films** were fabricated in our **homemade hot wall viscous flow vacuum MLD chamber** equipped with *in situ* Quartz Crystal Microbalance (QCM).

Each precursor was transferred into a bubbler to be introduced into the vacuum MLD chamber.

TMA, the ***inorganic precursor***, was held at room temperature due to its sufficient vapor pressure.

The ***organic precursors*** **BDO and BYDO**, were heated to 50 °C and 70 °C, respectively, to achieve reasonable vapor pressure.

B. Precursors and Reaction Condition

Inorganic Precursor	Organic Precursors	
	TMA (Trimethylaluminum)	BDO (1,4-Butanediol)	BYDO (2-Butyne-1,4-diol)
M.W.	72.09 g/mol	90.12 g/mol	86.09 g/mol
M.P.	15 °C	16 °C	53-58 °C
B.P.	125-130 °C	230 °C	238 °C
V.P.	20 mTorr (20 °C)	2 mTorr (85 °C)	0.56 mTorr (25 °C)

- To obtain **(–O–Al–O–$(CH_2)_n$–)$_i$ polymeric film**, Alucone MLD films were grown through **sequential reactions of TMA and with one of two diols different bond types (BDO or BYDO)** as the inorganic and organic precursors, respectively.
- The surface reactions for the alucone MLD films can be written as Equations (1) and (2):

(1) $-OH^* + Al(CH_3)_3 \rightarrow -O-Al-(CH_3)_2^* + CH_4$

(2) $-O-AlCH_3^* + OH(CH_2)_nOH \rightarrow -O-Al-O-(CH_2)_n-OH^* + CH_4$

Quartz Crystal Microbalance

A. Measuring Equipment

- **It is possible to measure the value of the fine mass change** according to the change of the frequency in conjunction with equipment Potentiostat + Galvanostat.
- This measuring equipment uses a quartz crystal which is a device for generating a continuous wave, resonance frequency.

B. Change of The Quartz Crystal Surface

- Before the deposition, quartz crystal vibrates mechanically with a constant frequency. When the deposition of reaction is started, the inorganic and organic precursors are deposited sequentially on the quartz crystal. And then, as **the quartz crystal mass is increased, the frequency is decreased at the same time.**
- **We can calculate the mass gain** of the deposited inorganic and organic precursors, respectively.

Result & Discussion

In-situ Analysis of Alucone MLD Film

Self-limiting Reaction

A. Saturation Curve (100 Cycles)

- The self-limiting reaction property of $(TMA/diol)_{100}$ alucone MLD film was confirmed by ellipsometer after MLD deposition with gradual increasing dose time of each precursor.
- The self-limiting reactions of BDO and BYDO with TMA at the surface were confirmed to obtain optimized conditions for alucone MLD growth.

B. Reaction Sequence

Sequence	1 Cycle					2 Cycle
Step	Step 1	Step 2	Step 3	Step 4	Step 1	...
(TMA/Diol)$_i$	TMA dose 3 s	Exposure 30 s	Purge 120 s	Evacuation30 s	TMA dose 3 s	...
	Step 5	Step 6	Step 7	Step 8	Step 9	...
	Diol dose X s	Exposure 30 s	Purge 120 s	Evacuation30 s	Diol dose X s	...

- TMA, BDO and BYDO were exposed over 3 s, 20 s and 60 s, respectively, without carrier gas. Then, the chamber was purged with a flow rate of 100 sccm for 2 min using Ar, and the chamber was evacuated for 20 s.
- **The binary MLD cycle** involves TMA dose then diol dose. Steps 1 to 8 consist of a single cycle.

Quartz Crystal Microbalance (QCM)

A. Mass Gain Curve for TMA/BDO films

B. Mass Gain Curve for TMA/BYDO films

Molecular ratio	TMA-BDO films	TMA-BYDO films
Early stage ($S_{CY.}$)	1 : 0.54	1 : 0.70
Latter stage ($S_{CY.}$)	1 : 0.34	1 : 0.62

- **The mass gains** in alucone films grown with varying doses of TMA and organic diol were identified by **quartz crystal microbalance (QCM) measurement.**
- TMA, BDO and BYDO were exposed over 5 s, 30 s and 60 s, respectively, without carrier gas and the precursors are exposured on the quartz crystal for 30 s. Then, the chamber was purged with a flow rate of 100 sccm for 60 s using Ar and had evacuation step for 5 min.
- In situ QCM mass gain curve after the TMA with BDO or BYDO surface reactions during **5 cycle in the early and last stage of alucone MLD film growth**. TMA is exposed onto Au quartz crystal as treated Al_2O_3 and BDO, BYDO is exposed after a saturation of TMA exposure.

Result & Discussion

Ex-situ Analysis of Alucone MLD Film

Film Thickness.

A. Depend on Chamber temperature

Chamber temperature (°C)	Thickness (nm)
80	28.5 ± 1.5
90	39.1 ± 1.6
100	20.5 ± 2.2
110	12.2 ± 3.5

- The thickness of $(TMA/BYDO)_{100}$ alucone MLD film was different depending on chamber temperature and the most thickest thickness showed at 90 °C.
- After having fixed the temperature, the experiment proceeds in accordance with the cycle for growth rate.

B. Growth rate

Cycle	(TMA/BDO) Thickness (nm)	(TMA/BYDO) Thickness (nm)
50	15.8 ± 1.2	19.8 ± 0.8
100	31.4 ± 2.0	39.1 ± 1.6
150	46.5 ± 3.0	58.7 ± 2.0
300	82.0 ± 6.5	118.8 ± 3.4

- Film thickness for $(TMA/BDO)_n$ alucone MLD films with various growth condition by controlling BDO dosing time and growth temperature measured by ellipsometry. The number of cycles is denoted as n.
- As BDO temperature is high and chamber temperature is low, the alucone MLD films is generally thicker depending on the cycle.
- The different tendency was discovered as different bond type of diol, such as BDO and BYDO, which have different slope with increasing cycles. This result implies that **more bigger bond type of diols leads to more increasing growth rate due to flexibility of precursor.**

Alucone MLD Film with Different Carbon Bond Type

Density Functional Theory (DFT)

A. Optimization of molecular geometry

- To confirm the intermolecular interaction and orientation between each of the molecules forming the alucone film, we designed the model as (TMA/diol), were chemisorbed on the most stable sites on Si (1 0 0) substrate.
- It implies the fact that the diol **with bigger bond type tends to vertical growth** between precursors due to low flexibility, which corresponds with the result of growth rate.

B. Double reaction

- Optimized molecular geometries of alucone MLD film after double reaction between TMA and two types of diol, BDO and BYDO on Si(100) surfaces for 1 cycle, which are obtained from DFT calculation.
- **The energy to need bending in (TMA/BDO) was less than (TMA/BYDO) bending energy.** These results indicate that the trend of increasing height with increased carbon bond type because of rigid bond from triple bond type.

Surface Potential and Roughness of Alucone MLD Film

A. NCM images

B. 2D SKPM images and Line profiles

- **Roughness of alucone MLD film** with different carbon bond type precursor. Two dimensional NCM images at the same locations of SKPM images in MLD alucone films.
- **Surface potential of alucone MLD film** with different carbon bond type precursor. Two dimensional SKPM images, line profiles and histogram at 0-3 V of (c) $(TMA/BDO)_{100}$ normal condition (d) $(TMA/BYDO)_{100}$ normal condition grown on Si(100) wafers for 100 cycles.
- **The $(TMA/BYDO)_{100}$ alucone MLD film** showed a **relative homogeneous surface** with line profiles.

Summary

We have fabricated organic-inorganic alucone polymeric film by MLD, which can be obtained by optimized conditions such as surface saturation, using between trimethylaluminum (TMA) and one of two diols with different carbon-carbon bond order as inorganic and organic precursors, respectively. The surface chemistry and self-limiting reactions, which are properties of MLD, were confirmed by ellipsometer after deposition by our homemade MLD chamber. The mass gains in alucone films grown with varying doses of TMA and organic diol were identified by quartz crystal microbalance (QCM) technique. In addition, the growth rate of the alucone MLD film showed different aspects in the characterization result due to molecular flexibility of each organic precursor. All molecular geometries and energies were predicted by performing density functional theory (DFT) calculations.

Reference

1. "Synthesis of Zeolite As Ordered Multicrystal Arrays." J. S. Lee, Y. -J. Lee, E. L. Tae, Y. S. Park, K. B. Yoon, *Science*, **2003**, 301, 818–821.
2. "Molecular Layer Deposition of Alucone Polymer Films Using Trimethylaluminum and Ethylene Glycol." A. A. Dameron, D. Seghete, B. B. Burton, S. D. Davidson, A. S. Cavanagh, J. A. Bertrand, S. M. George, *Chem. Mater.* **2008**, *20*, 3315–3326.
3. "Fine-Tunable Absorption of Uniformly Aligned Polyurea Thin Films for Optical Filter using Sequentially Self-Limited Molecular Layer Deposition" Y.-S. Park, S.-E. Choi, H. Kim, J. S. Lee*, *ACS Applied Materials & Interfaces*, **2016**, 8 (18), 11788–11795.
4. "Intramolecular and Intermolecular Interactions in Hybrid Organic–Inorganic Alucone Films Grown by Molecular Layer Deposition"

E

Introduction

We focus on plasma synthesis of hybrid nanomaterials based on vertically oriented graphene and their application on energy storage, biomedicine, catalysis, biosensors.

These hybrids were obtained by PECVD after periodic changes of the deposition parameters to trigger various growth regimes [1-3], or by post-synthesis decoration. For decoration of Carbon Nanowalls (CNW) or vertically graphene we used: Electro-Deposition (ED); plasma functionalization; and decoration with particles by magnetron sputtering (MS) & cluster source [4].

The characteristics of these hybrid nanostructures were investigated by SEM, HRTEM, Raman, XPS and cyclic voltammetry.

Experimental set-up for CNW synthesis, functionalization and their characteristics [1-3]

Deposition of CNW

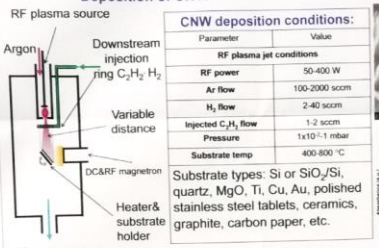

CNW deposition conditions:

Parameter	Value
RF plasma jet conditions	
RF power	50-400 W
Ar flow	100-2000 sccm
H_2 flow	2-40 sccm
Injected C_2H_2 flow	1-2 sccm
Pressure	1x10^{-1}-1 mbar
Substrate temp	400-800 °C

Substrate types: Si or SiO_2/Si, quartz, MgO, Ti, Cu, Au, polished stainless steel tablets, ceramics, graphite, carbon paper, etc.

Characteristics of as-deposited CNW

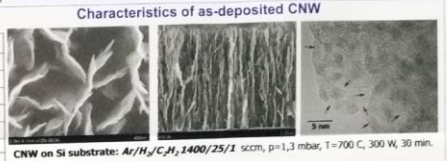

CNW on Si substrate: *Ar/H_2/C_2H_2 1400/25/1* sccm, p=1,3 mbar, T=700 C, 300 W, 30 min.

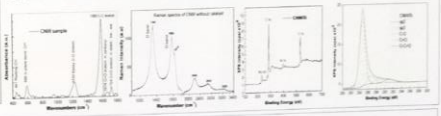

i) Hydride nanostructures fiber/CNW; CNW/fiber; CNW/CNW by switching temperature and CNW/W-clusters by cluster source

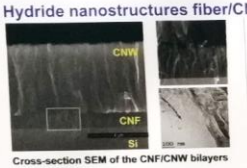

Cross-section SEM of the CNF/CNW bilayers

SEM of hybrid by successive depositions conditions (temp. 700 °C/200 °C)

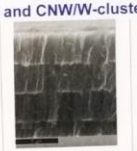

Cross SEM CNW/CNW

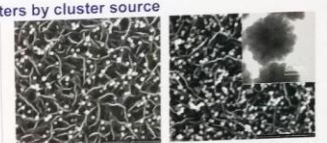

SEM of CNW decorated with W clusters [4] obtained after 20 and 60 s

ii) Decoration of CNW with RuO_2 nanoparticles for supercapacitor [5] (collaboration with CNRS, LAAS, Toulouse, France and INRS-Énergie, Matériaux, Québec, Canada)

Diagram of CNW/hRuO2 hybrid electrode

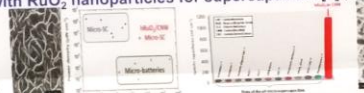

Capacitance of CNW/hRuO$_2$ and other nanostructures.

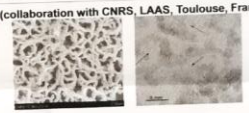

SEM and TEM of CNW/RuO$_2$ on CNW

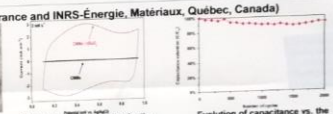

Electrochemical characterization CNW and CNW/hRuO$_2$ electrode.

Evolution of capacitance vs. the number cycles at 1.5 mAcm^2.

iii) Decoration of CNW and functionalized CNW with sputtered Pt for catalysis, biosensor and fuel cells

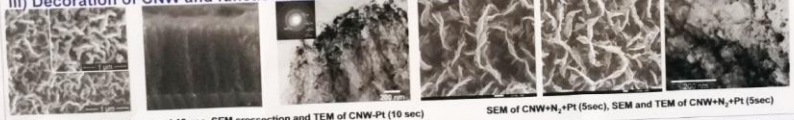

SEM of CNW+Pt: 30s - inset and 10 sec, SEM crossection and TEM of CNW-Pt (10 sec)

SEM of CNW+N_2+Pt (5sec), SEM and TEM of CNW+N_2+Pt (5sec)

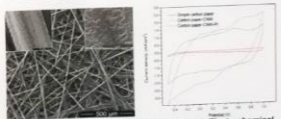

Morphology of CNW on Carbon Paper (CP) and Electrochemical characterization of CP, CNW@CP and CNW+Pt@CP.

iv) Decoration of CNW+(CeO_2 and Ag) for enhancement cells adhesion and proliferation, and bactericidal surfaces

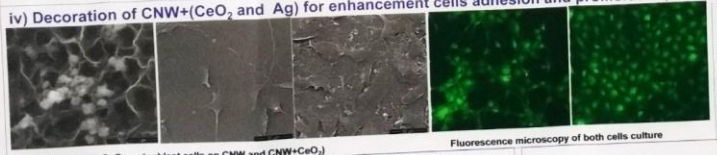

SEM of CNW+CeO_2, osteoblast cells on CNW and CNW+CeO_2

Fluorescence microscopy of both cells culture

SEM image of Pseudomonas aeruginosa on (a)-Ti (normal morphology & adhesion) (b) –on CNW and (c)- on CNW+Ag (non adherence, membrane damaged/altered)

v) Decoration of CNW+SnO sensors and Au for SERS detection

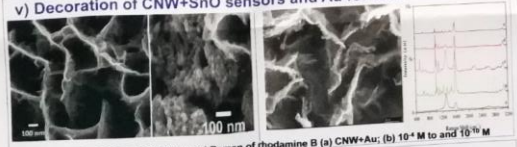

SEM of CNW:SnO_2 [6] and CNW+Au and Raman of rhodamine B (a) CNW+Au; (b) 10^{-4} M to and 10^{-10} M

Conclusions

- ✓**We obtained hybrid nanomaterials from vertically graphene combined with nanofibres or nanoparticles (RuO_2, CeO_2, Pt, Au, Ag, W etc) by simultaneous or sequential PACVD, PVD and e-chemistry;**
- ✓**CNW layers are suitable as electrode in batteries and supercapacitors. These interconnected networks of 2D-graphene nanostructures, exhibited a good electrochemical response towards the redox reactions which can be increase after decoration;**
- ✓**CNW decorated with $hRuO_2$ particles offers an exceptional potential for micro-supercapacitors that can compete in terms of specific energy density with micro-batteries;**
- ✓**By adjusting the experimental conditions for the synthesis of CNW layers and electro-deposition parameters for $hRuO_2$, we obtained remarkable specific capacitance of ~ 1.1 F/cm^2, which is three orders of magnitude higher than those obtained in the case of micro-supercapacitors based on graphene [5];**
- ✓**Plasma jet functionalization introduce new chemical groups at CNW surface and lead to homogeneous dispersion of nanoparticles over walls surface;**
- ✓**The cyclic voltammograms showed that the electrochemical activity increases after decoration of CNW with nanoparticles, obtaining high performance hybrid electrodes for electrochemistry. The results present possibility of utilization of CNW in for biosensors, batteries and membranes for fuel cells;**
- ✓**In biology: increasing of adherence of osteoblast cultures was observed on CNW decorated with CeO_2.**
- ✓**The bactericide behavior of CNW edge that penetrate bacteria membrane were enhanced after CNW decoration with Ag;**
- ✓**Decoration with gold clusters lead to high sensitive SERS platforms, while after decoration with W or SnO_2 [6] high performance gas sensor could be fabricated.**

References

1. Vizireanu, S; Nistor, L; Haupt, M; Katzenmaier, V; Oehr, C; Dinescu, G. "Carbon nanowalls growth by radiofrequency plasma-beam-enhanced chemical vapor deposition"; PLASMA PROCESSES AND POLYMERS (5) 3 263-268 (2008).
2. Vizireanu, S; Stoica, S. D; Luculescu, C; Nistor, L. C; Mitu, B. Dinescu, G. "Plasma techniques for nanostructured carbon materials synthesis. A case study: carbon nanowall growth by low pressure expanding RF plasma"; PLASMA SOURCES SCI. & TECHNOLOGY (19) 3 (2010).
3. Vizireanu, S; Mitu, B; Luculescu, C; Nistor, L; Dinescu, G. "PECVD synthesis of 2D nanostructured carbon material"; SURFACE & COATINGS TECHNOLOGY (211) 2-8 (2012).
4. Acsente, T., Negrea, R.F., Nistor, L.C., Logofatu, C., Matei, E., Birjega, R., Grisolia, C., Dinescu, G., Synthesis of flower-like tungsten nanoparticles by magnetron sputtering combined with gas aggregation, European Physical Journal D 69: 1239 (2015).
5. Dinh, T.M., Achour, A., Vizireanu, S., Dinescu, G., Nistor, L., Armstrong, K., Guay, D., Pech, D., Hydrous RuO2/carbon nanowalls hierarchical structures for all-solid-state ultrahigh-energy-density micro-supercapacitors, NANO ENERGY (10) 288-294 (2014).
6. Palla-Papavlu, A., Filipescu, M., Vizireanu, S., Vogl, L., Antohe, S., Dinescu, M., Wokaun, A., Lippert, T., Laser-induced forward transfer of hybrid carbon nanostructures, Applied Surface Science 374, 312-317 (2016).

Acknowledgement: This work was partially supported by the Romanian Ministry of Education and Research under Nucleus programme-contract 4N/2016, contract PN-II-PTPCCA-2013-4-0473 and PN-III-P2-2.1-PED-2016-0287.

F

Introduction

Oil pollution caused by oily industrial wastewater and frequent oil spill accidents has become one of the most urgent global environmental problems.

by *Wikipedia* by *The Times*

Recently, materials with extreme wettability have attracted increased attention for oil/water separation, e.g., fish scales inspired in-air-superhydrophilic & underwater-superoleophobic materials.

(*Adv. Mater.* 6/2009)

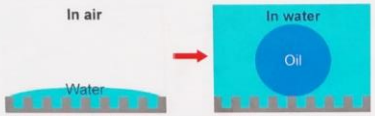

Superhydrophilic in air

Superoleophobic in water

Though many methods have been proposed to fabricate materials with superwettability, most of the methods involve corrosive or toxic chemicals which will cause new environmental concerns.

Objective

Develop a facial, environment-friendly method to fabricate super-wetted mesh for effective oil/water separation.

Fabrication of super-wetted nylon mesh

Helium atmospheric pressure plasma jet (APPJ) was used to functionalize nylon mesh. Then the mesh became superhydrophilic in air and superoleophobic in water. Water can be quickly absorbed by the mesh in air, while oil droplet can hardly be adhered by the mesh in water.

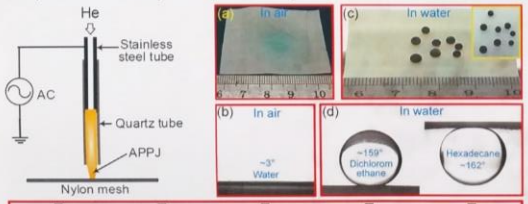

大连理工大学 DALIAN UNIVERSITY OF TECHNOLOGY

UCL

Wettability with different APPJ treatment time

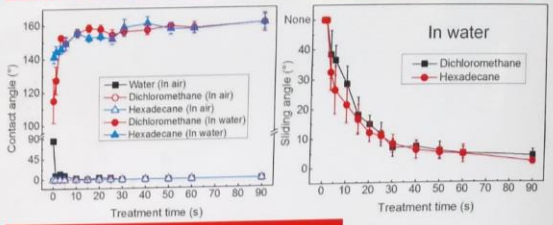

Morphology and composition

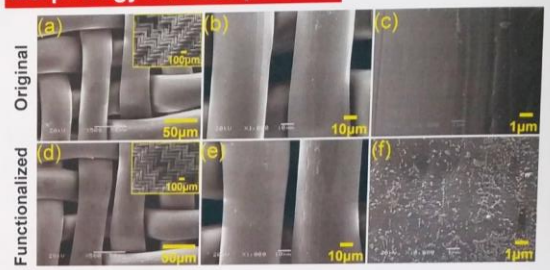

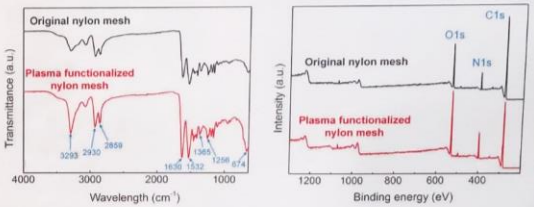

SEM, FTIR and XPS results demonstrated that micro-/nanostructures and oxygen-containing groups were created on the nylon fibers.

Oil/water separation

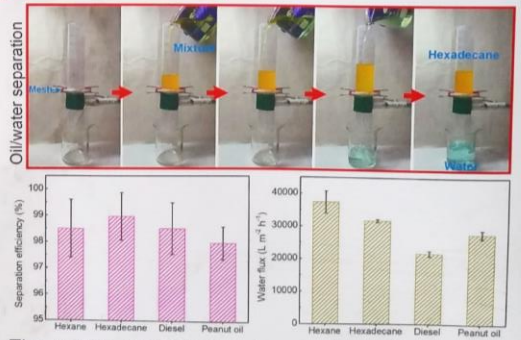

The water pre-wetted nylon mesh could separate various oil/water mixtures with high efficiency (>97.5%) and water flux (> 20000 L/m²h). Results also demonstrated that the functionalized nylon mesh has excellent recyclability and durability.

G

Silicon nitride is electronically neutral and nonporous so that noncovalent functionalization by physical interactions is hampered. This together with its great chemical inertness makes new modifications highly required widen its feasibility. In this sense, we point out poydopamine modification as a straightforward strategy that would make the further surface functionalization possibilities easier since polydopamine can be directly react with amine o thiol molecules. The polydopamine modification is a process bio-inspired by the mussel-chemistry. **Polydopamine coating is obtained by dopamine oxidative self-polymerization in a basic medium(pH=8.5**

SEM CHARACTERIZATION

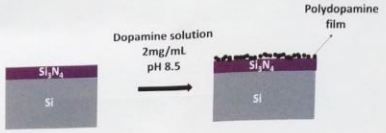

RAMAN CHARACTERIZATION

The success in the polydopamine coating was corroborated by Raman spectroscopy, Figure

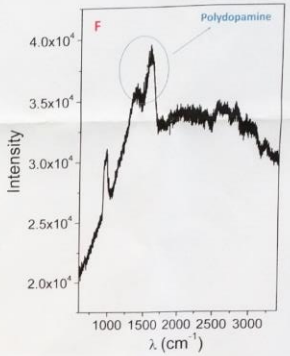

Figure 1. A) SEM Image of the top surface and the perpendicular section of the silicon nitride wafer; B, C and D) SEM Images considering the top surface and the perpendicular section of the silicon nitride wafer after the polydopamine polymerization. F) Raman spectrum of the silicon nitride surface after polydopamine modification.

WATER CONTACT ANGLE

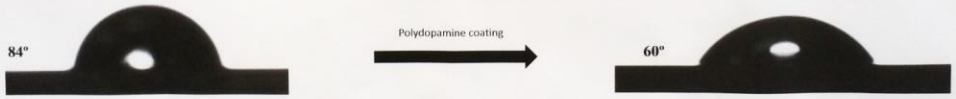

Figure 2. Water contact angles: Left) Silicon nitride surface and Right) silicon nitride coated with a polydopamine film.

AFM CHARACTERIZATION

Figure 3. A and B) AFM images (2 and 3D) for the silicon nitride surface after poydopamine modification. Frame dimensions: 5μm × 5μm. C) Analysis of the roughness

CONCLUSIONS:

Poolished Silicon nitride surface can be easily modified with a thin film of polydopamine. The topography of surface was studied by SEM and AFM: The film consisted in a polydopamine cement with a large amount of aggregates of polydopamine nanoparticles dispersed along the surface.

After polydopamine modification: the silicon nitrides become more hydrophilic (60°) and more rough (mean square roughness of 23.6 nm).

What did the teachers (VJ, SF) think?

(Note, we graded independently (in 2019 so we might not remember exactly), but we had discussed the posters before when selecting from a bigger list)

Overall, I would say that we were largely in agreement on which posters were good and which slightly less so. My (VJ) average score was much higher.

There is a bigger discrepancy in the posters that stray the furthers from the norm (B, C, E) since the rubric becomes difficult to use. However, in these cases we are still in full agreement about the overall quality of the poster, just disagree exactly where in the rubric this is reflected.

A

VJ
Structure: 4
Effort: 4

SF
Structure: 3
Effort: 2

-Good poster
-Some ”floating” elements

MOTIVATION

- The intriguing intrinsic photoluminescence (PL) of gold nanoparticles (AuNPs) has received increasing attention over the last years due to potential applicability in a great number of biosensing, imaging or optical labelling applications [1,2].
- The nonbleaching nature of their PL signal, strongly correlated with plasmon resonances and size, enables their probing by fluorescence spectroscopy techniques, such as fluorescence correlation spectroscopy (FCS) toward label-free sensing applications.
- Despite several available reports, the field of PL - based biosensing applications using FCS, remains partially unexplored, due to incomplete elucidation of the mechanism behind PL.

GOALS

- Investigate the PL and diffusion behavior of AuNPs of spherical/rod-like shape and different sizes, in solution, by performing one-photon excited FCS assays under excitation at 405 nm (interband transition of gold).
- Extract the diffusion parameters by fitting the obtained PL autocorrelation curves.
- Correlate the hydrodynamic diameter of the AuNPs obtained using Stokes-Einstein equation with results obtained from transmission electron microscopy (TEM) and dynamic light scattering (DLS).

SAMPLES AND INSTRUMENTATION

A. Gold nanospheres (AuNSs) stabilized with cetyltrimethylammonium chloride (CTAC)
B. Gold nanorods (AuNRs) stabilized with cetyltrimethylammonium bromide (CTAB)

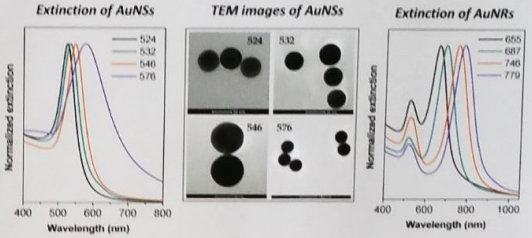

FCS measurements:
- MicroTime200 confocal fluorescence system equipped with Olympus IX71 microscope
- Pulsed excitation provided by **405 nm laser diode** (40 MHz, 40 µW)
- Two SPAD detectors for cross-correlation analysis
- 60×/1.2-NA objective, 430LP emission filter and 150 µm pinhole
- ***Fluorescence Lifetime Correlation Spectroscopy (FLCS) analysis***

DLS measurements:
- Zetasizer NanoZS90 instrument (Malvern Instruments) equipped with a He-Ne laser (633 nm, 5 mW).

Gold nanospheres

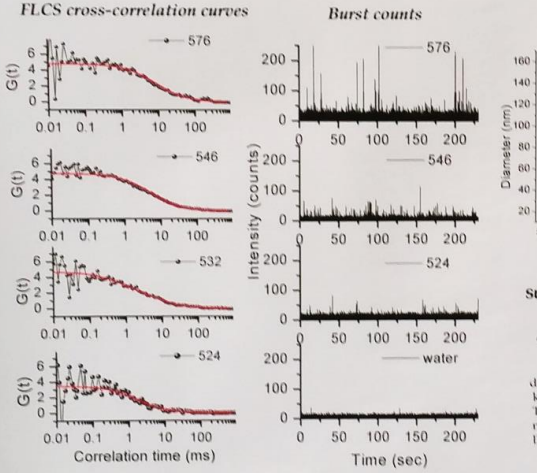

Stokes Einstein Equation

$$d_{FCS} = \frac{kT}{3\pi\eta TD}$$

d_{FCS} = hydrodynamic diameter
k = Boltzmann constant
T = temperature
η = solvent viscosity
D = diffusion coefficient

Gold nanorods

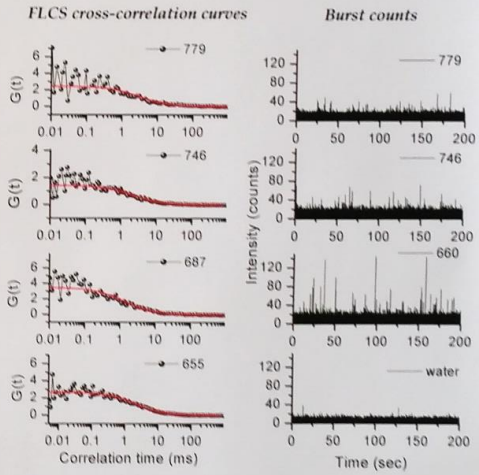

Sample	$\langle\tau_d\rangle$* (ms)	$\langle D\rangle$** (µm²/sec)	$\langle d_{FCS}\rangle$ (nm)	$\langle d_{TEM}\rangle$ (nm)	$\langle d_{DLS}\rangle$ (nm)
AuNSs 524 CTAC	1.7	16	30.4	22	71
AuNSs 532 CTAC	4.2	6.4	76	58.7	84
AuNSs 546 CTAC	5.4	5.2	93.6	81.5	115
AuNSs 576 CTAC	8	3.6	135.2	112	158

* diffusion time; ** diffusion coefficient

Sample	$\langle\tau_d\rangle$ (ms)	$\langle D\rangle$ (µm²/sec)	$\langle d_{FCS\text{-}orthi}\rangle$ (nm)	$\langle d_{DLS}\rangle$ (nm)
AuNRs 655	2.2	12.4	39.2	51
AuNRs 687	1.4	20	24.3	33
AuNRs 746	2.3	11.8	41.2	54
AuNRs 779	3.2	8.5	57.3	68

* diffusion time; ** diffusion coefficient

GENERAL CONCLUSIONS

- *Spherical and rod-shaped AuNPs exhibiting intrinsic PL at 405 nm excitation were successfully characterized by FLCS in water solution*
- *The diffusion parameters extracted from cross-correlation analysis using FLCS filters are well strongly related to the size of the diffusing AuNPs.*
- *Hydrodynamic diameters obtained from FCS were compared with values obtained by TEM and DLS*
- *The results obtained here make us confident that by combining the PL properties of AuNPs with the highly sensitive FCS method, reliable label-free sensitive detection methods can be developed.*

B

VJ
Structure: 2
Effort: 4

SF
Structure: 1
Effort: 1

-Extreme text overdose
-Opinions on amount of text differ, but this is too much

INTRODUCTION

Three-dimensional (3D) cell culture is an emerging practice in various applications such as drug discovery, disease modelling and stem cell research. Traditional 2D cell culture models are lacking normal interactions between the cells and extracellular matrix (ECM). As a consequence, several problems may occur. For example, pre-clinical drug discovery studies with 2D cultured cells can result in biased results and improper conclusions, which may lead to expensive failures at the later stages of the drug development. 3D culturing of the cells results in more natural growth and improved functionality as 3D culturing resembles *in vivo* micro-environment better. Hydrogels are most common way to culture cells in 3D. Nanofibrillar cellulose (NFC) hydrogel (GrowDex®) has been successfully used in 3D culture of different cell types.

GrowDex is wood-based NFC hydrogel developed for 3D cell culture **(Fig 1.)**. It is biocompatible with human cells and tissues but as a plant based product it does not contain any animal or human derived material. GrowDex efficiently supports 3D cell growth by physically resembling extracellular matrix ECM (1,2,3). The structure and mechanical properties of GrowDex can be tuned to fulfill the requirements of different cell types and it allows the diffusion of nutrients and oxygen.

Under stress GrowDex has shear thinning properties, which make it a pipettable ready-to-use hydrogel.

Figure 1. GrowDex hydrogel.

One of most interesting properties of GrowDex is the **possibility to degrade the hydrogel by cellulase enzyme treatment**, while retaining the grown 3D cell structure. This is important in applications where the grown 3D cell structures are utilized and analyzed in various downstream processes, such as detailed imaging of 3D cell surface (4).

To deepen our knowledge about NFC hydrogel degradation process, a real-time analysis method was developed to observe the degradation kinetics. Various cellulase enzymes were used in concentration series. Additionally, the effect of cellulase enzymes on cell viability was studied *in vitro* with two cell lines.

AIMS OF THE STUDY

1. Develop and optimize a **real-time assay for the analysis of enzymatic degradation** of nanofibrillar cellulose hydrogel
2. Study the degradation **with various cellulase enzymes**
3. Test the **effect of enzyme treatment on cells *in vitro***

MATERIALS AND METHODS

Materials

- GrowDex® hydrogel (UPM, Finland)
- Purified cellulase enzyme mixture (UPM), and cellulase enzymes from *Aspergillus niger*, *Trichoderma viride*, and *Trichoderma Reesei* (Sigma-Aldrich)
- HepG2 and WA07 cells with culturing medium and supplements

Analysis methods

Nephelometry analysis

Enzymatic degradation of nanocellulose hydrogel was detected with nephelometry technique that measures light scattering in real time (Nepheloskan Ascent, Labsystems, Finland). GrowDex was diluted to 0.7% with PBS. Different enzyme concentrations were prepared by diluting enzyme stock solutions to desired concentrations with PBS (0–500 µg/mg cellulose with UPM enzyme and 0-200 U/ml with Sigma enzymes), respectively. Degradation studies were performed in 96-well format: 100µL of the hydrogel was transferred to 96-well plate (Brandplates pureGrade, Brand GMBH, Germany) and 100µL of cellulase enzyme was added on top of the hydrogel. Immediately after adding the enzyme, the plate was sealed with transparent adhesive film (ThermalSeal RT, Sigma-Aldrich) to prevent evaporation, and the experiment was carried out at 37°C. GrowDex degradation with different enzyme treatments was measured over 24h without shaking and with 60 RPM shaking, respectively.

Determination of glucose

Cellulase enzymes degrade cellulose to glucose mono units. Determination of glucose from degraded GrowDex samples by 3,5-dinitrosalisylic acid (DNS) –assay (5) was performed as a secondary assay after the nephelometry experiments. DNS reacts with reducing sugars, and it is reduced to to 3-amino,5-nitrosalisylic acid, which can be quantified by spectrophotometry. Samples and glucose standard solutions (100µL) were mixed with DNS reagent (150µL) and placed into boiling water for 5 min. The reaction was stopped by placing the samples on ice, 100µL was transferred into 96-well plate (Brandplates pureGrade), and absorbance was measured at 540nm with spectro-photometer (iEMS Reader MF, Thermo Electron Corporation, Finland).

***In vitro* cell cultures**

The effect of the cellulase enzymes on cell viability was examined in vitro **2D cell cultures** with two different cell lines, **HepG2** (HB-8065™, ATCC, VA, USA) and **WA07** (Wicell, WI, USA). For cell viability and growth study, HepG2 cells were seeded in 200 µL

MATERIALS AND METHODS (continued)

on 96-well plate (Nunclon Sphera™, ThermoFisher Scientific). WA07 cells were seeded on Matrigel –coated 96-well plate. After 24 h incubation at 37°C in 5% CO_2, different enzyme concentrations in culture medium were administered to the cells and incubated at 37°C for 24h. **AlamarBlue assay** (ThermoFisher Scientific) was performed prior to and after the enzyme treatment to study the effect of enzyme on the mitochondrial metabolic activity of the cells. Additionally, the effect of cellulase enzyme to **3D cell cultures** in GrowDex was analyzed. HepG2 cells were cultured 3D in 0.8% GrowDex by seeding 600 cells/µl in 100µl hydrogel to Ultra-low attachment 96 well plate (Corning Costar®) and adding 100µl of supplemented culture medium on top. AlamarBlue assay was performed prior to, and after the enzyme treatment. **Live/Dead assay** was performed using calcein-AM for live cells and ethidium homodimer-1 for dead cells.

RESULTS

A clear concentration-dependent kinetics was observed with UPM cellulase enzyme and with cellulase from *Trichoderma Viride* in nephelometric real-time analysis of GrowDex degradation *(Fig 2A and B)*. The light scattering from cellulose nanofibers decreases as the fibers are degraded to soluble sugar molecules. On the contrary, cellulase from *Aspergillus Niger* did not show similar degradation profile (Fig 2C). The result is likely due to different enzymes present in the enzyme products. The shaking of plate during the experiment did not have effect on the degradation speed (data not shown). It was observed that *Trichoderma Viride,* and especially *Aspergillus Niger* enzymes contain glucose, which induced a bias in glucose determination analysis (Fig 2B and C). UPM enzyme does not contain glucose, and degradation resulted in equal glucose amounts with enzyme concentration 100mg/g and above (Fig 2A), suggesting full degradation of cellulose nanofibers.

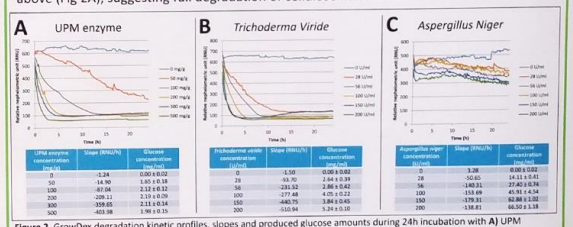

Figure 2. GrowDex degradation kinetic profiles, slopes and produced glucose amounts during 24h incubation with **A)** UPM cellulase enzyme **B)** Cellulase from *Trichoderma Viride* and **C)** Cellulase from *Aspergillus Niger.*

The effect of UPM cellulase (Fig. 3A) and *Trichoderma Reesei* cellulase (Fig. 3B) on cell viability was examined *in vitro* 2D cell cultures of HepG2 and WA07. It was observed that both cells tolerate 24h enzyme treatments well. The mitochondrial activity was not significantly changed when different enzyme concentration were tested. Slight decrease in viability was seen when highest enzyme concentration were used. This may be related to decreased culture medium content during the incubation with enzyme. HepG2 spheroids cultured 3D in GrowDex showed also good viability after enzymatic removal of GrowDex (Fig. 4). Only few dead cells were observed with Live/Dead staining after 24h incubation with high enzyme concentration (500mg/g), and also AlamarBlue analysis showed good tolerance for cellulase treatment.

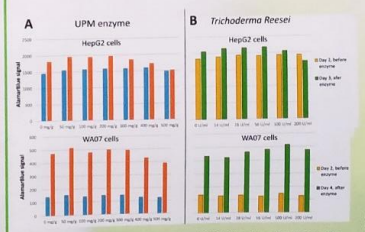

Figure 3. Mitochondrial activity of HepG2 and WA07 2D cultured cells after 24h treament with **A)** UPM cellulase and **B)** *Trichoderma Reesei* cellulase enzymes.

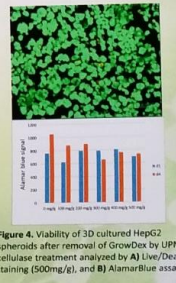

Figure 4. Viability of 3D cultured HepG2 spheroids after removal of GrowDex by UPM cellulase treatment analyzed by **A)** Live/Dead staining (500mg/g), and **B)** AlamarBlue assay

DISCUSSION AND CONCLUSIONS

Degradation of 3D culturing matrix is beneficial in various applications. As human cells do not contain cellulose, cellulase enzyme can be used to remove GrowDex hydrogel without harming the cells. Light-scattering method is convenient method for real-time analysis of cellulose fiber degradation kinetics. Commercial cellulase products contain different amounts of cellulase enzymes such as endoglucanase and β-glucosidase, and impurities that may have an affect on the degradation process.

C

VJ
Structure: 4
Effort: 2

SF
Structure: 3
Effort: 1

-Poster seriously lacks data.
-This poster is almost ”all structure, no content”

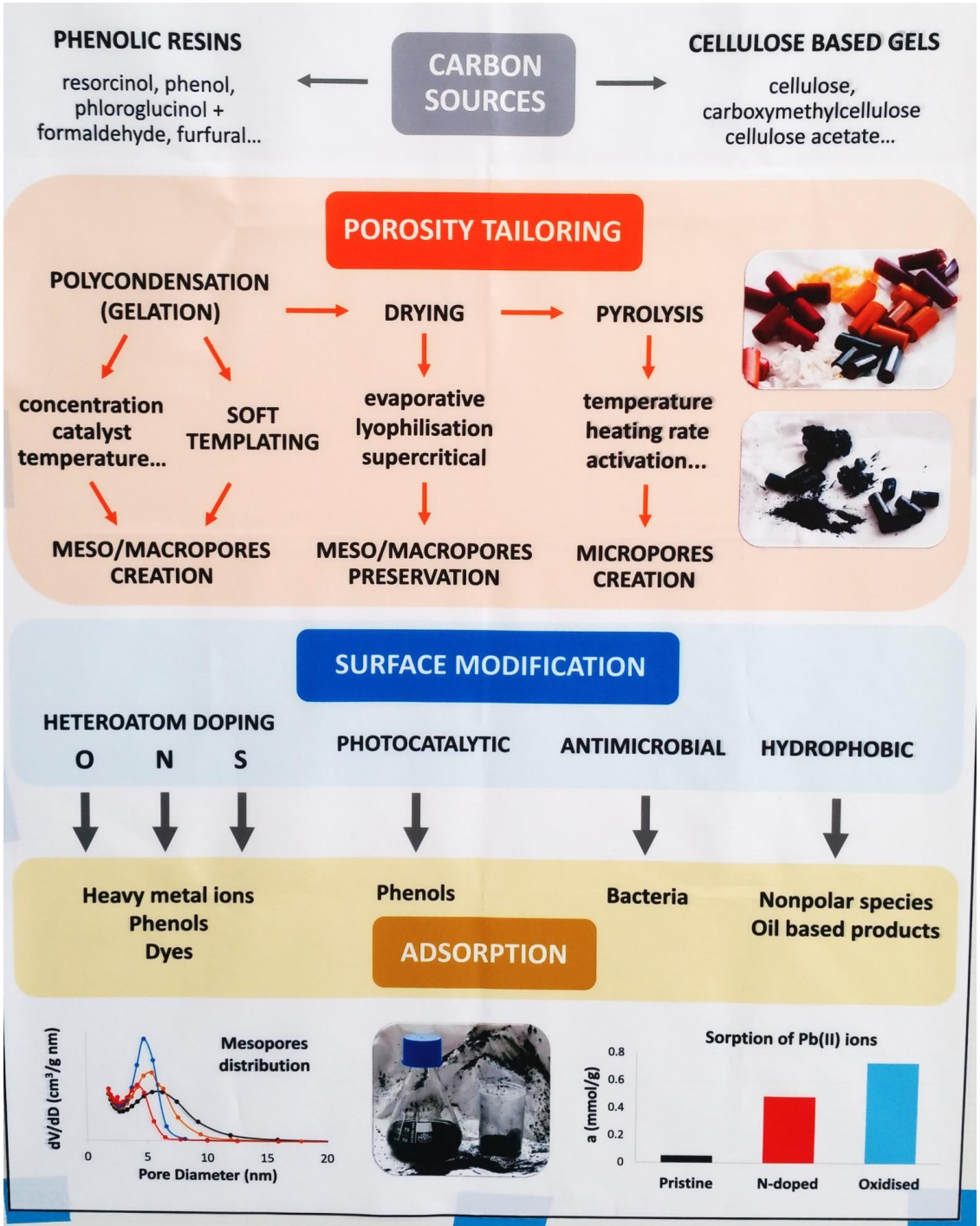

D

VJ
Structure: 2
Effort: 5

SF
Structure: 1
Effort: 3

-Suffers from data overload!
-Could be great if >50% of content was cut.

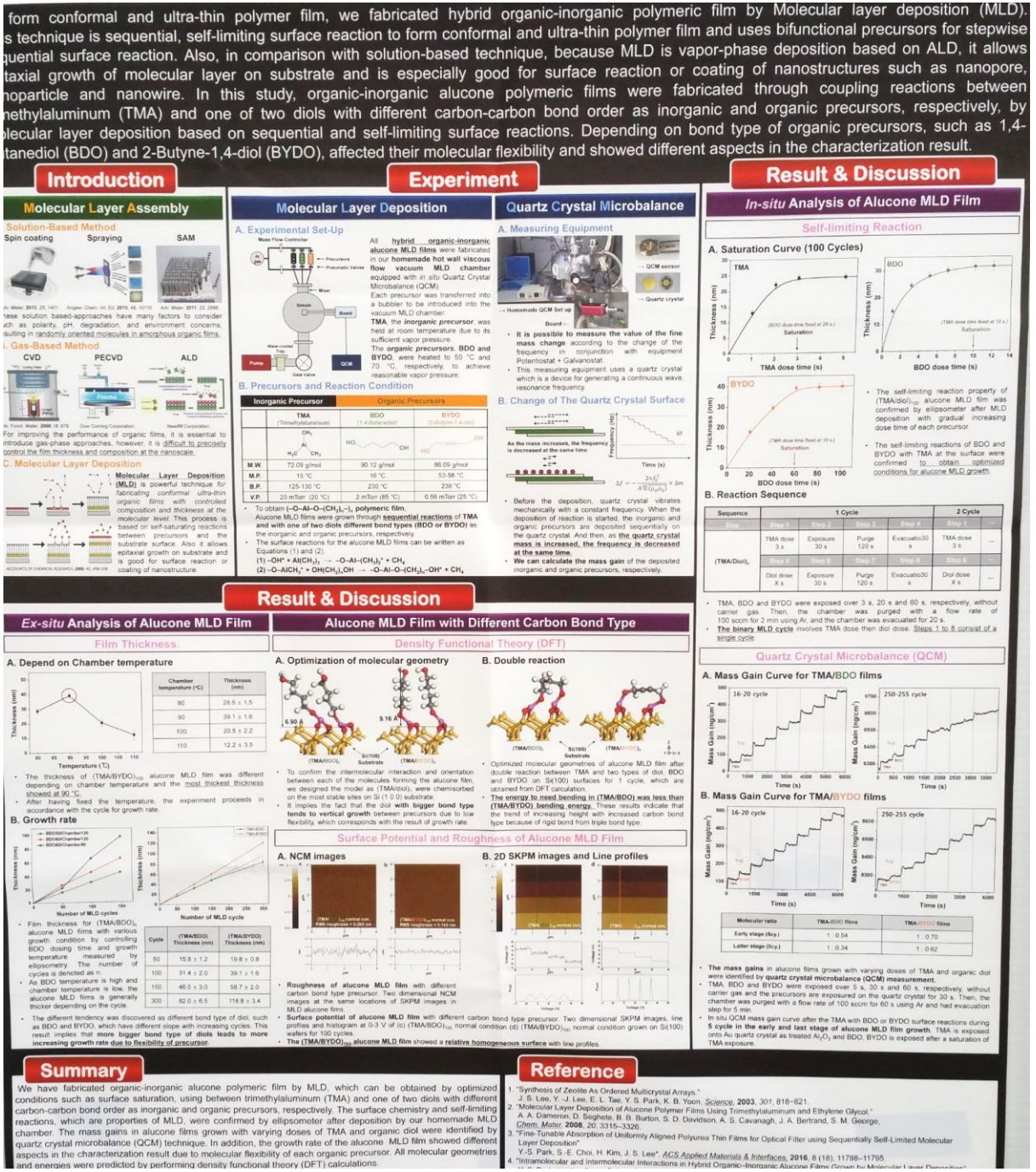

E

VJ
Structure: 1
Effort: 3

SF
Structure: 1
Effort: 2

-This poster almost completely lacks structure.
-It is the opposite problem to poster C

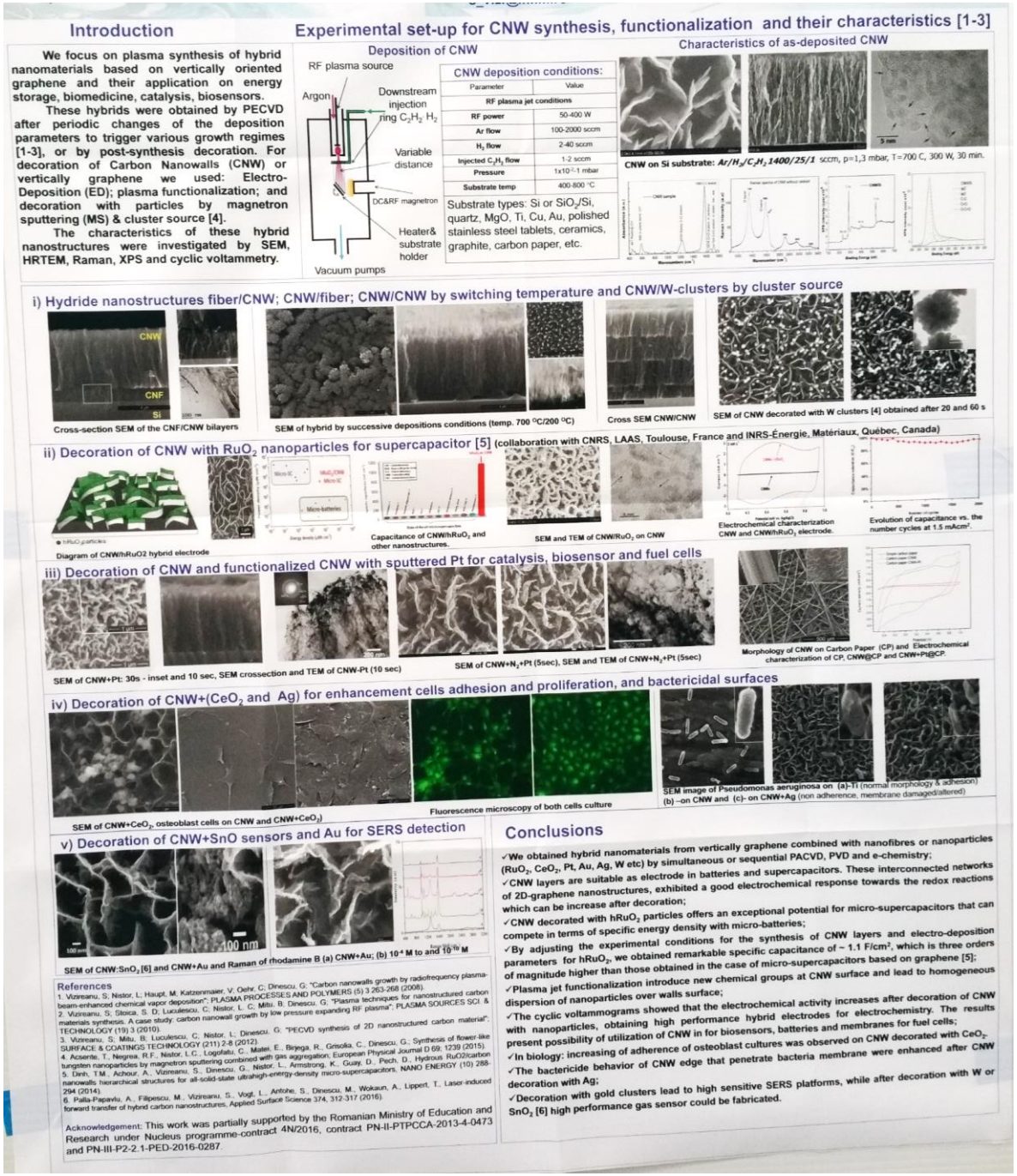

F

VJ
Structure: 4
Effort: 5

SF
Structure: 4
Effort: 4

- Our consensus for the best poster.
- Good balance of data, images, text.
- Clear structure, with simple but appealing colour theme.

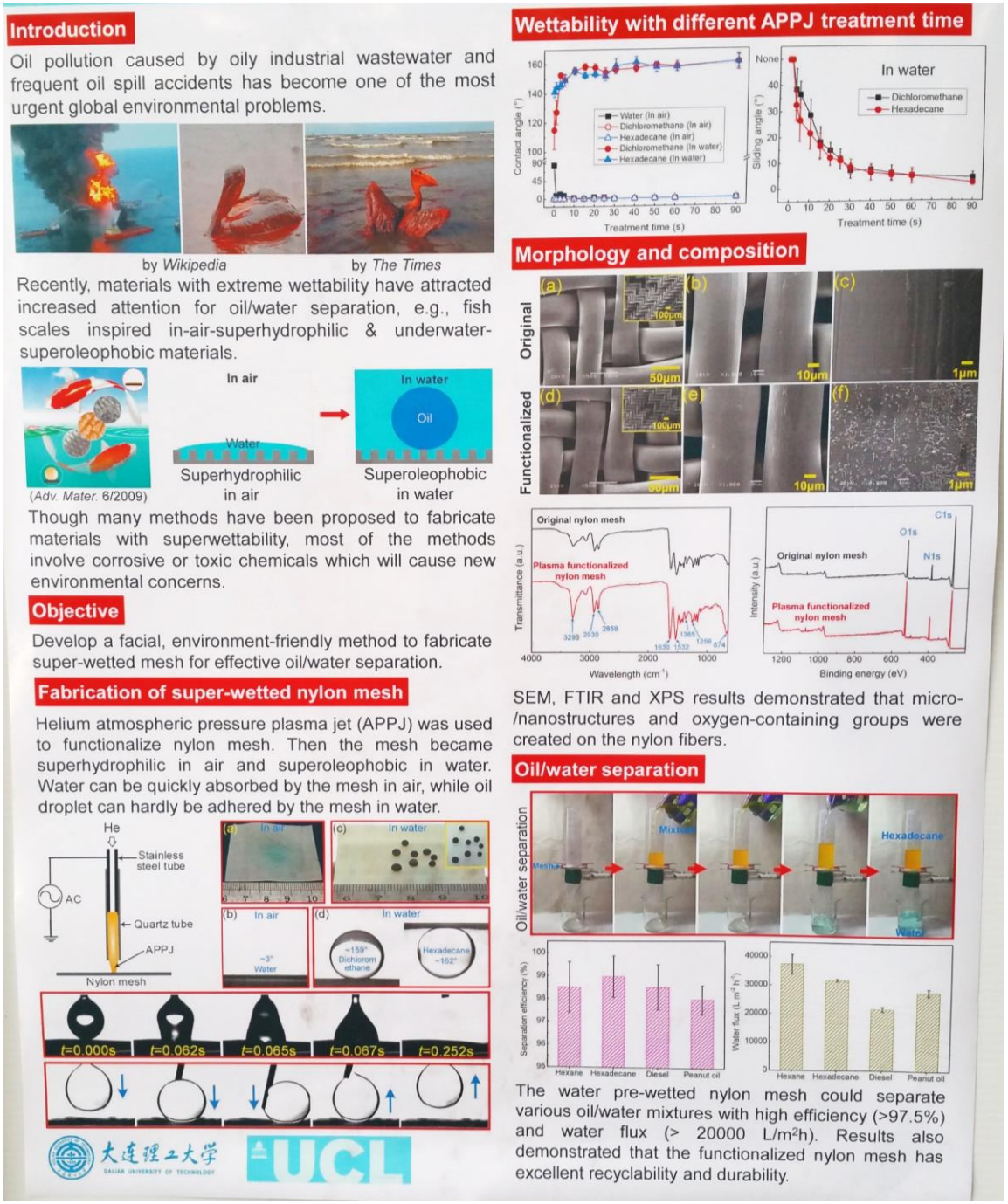

G

VJ
Structure: 3
Effort: 1

SF
Structure: 2
Effort: 1

- There is data, there are images, and there is some text.
- But it looks very unfinished.

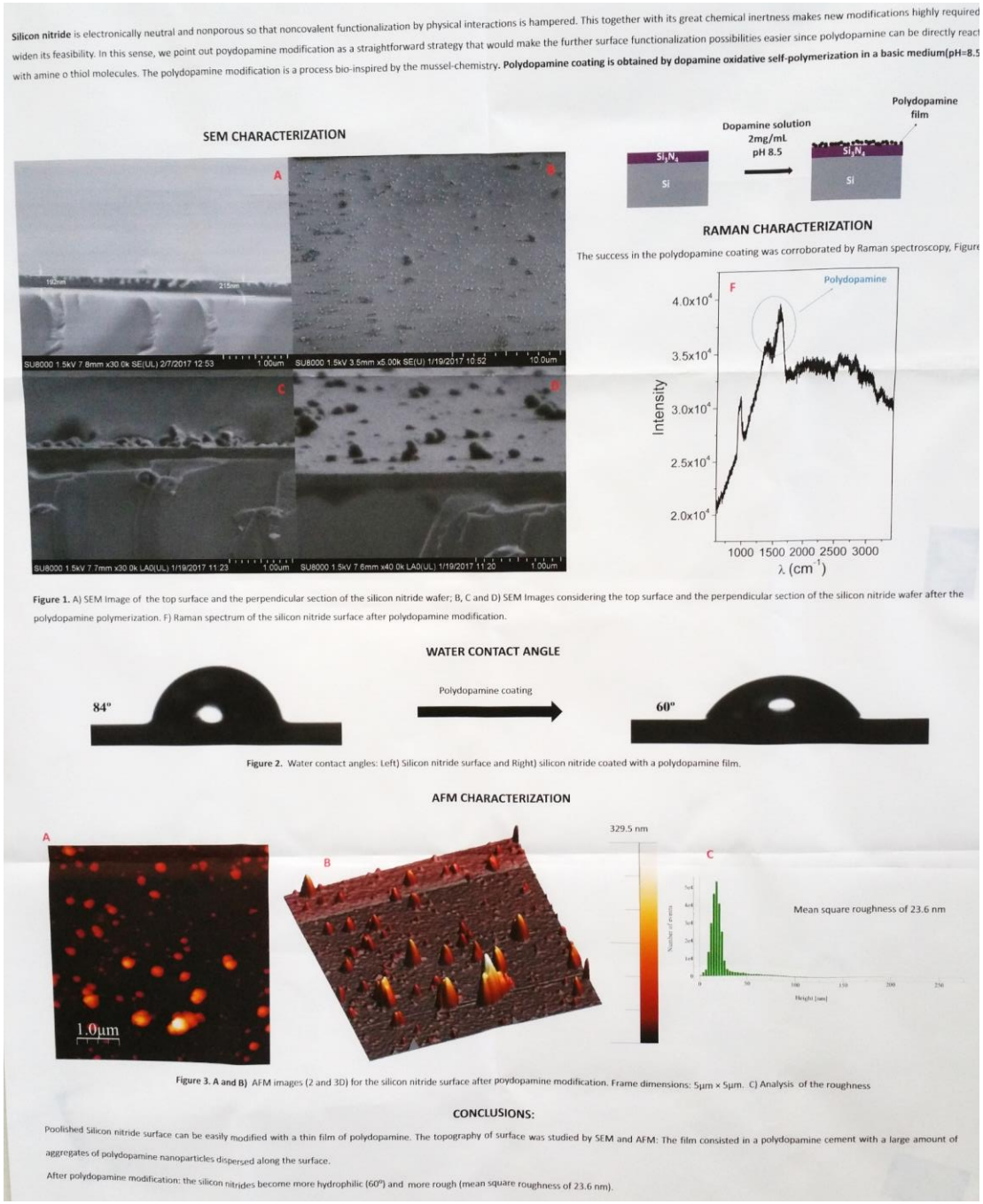

Silicon nitride is electronically neutral and nonporous so that noncovalent functionalization by physical interactions is hampered. This together with its great chemical inertness makes new modifications highly required widen its feasibility. In this sense, we point out poydopamine modification as a straightforward strategy that would make the further surface functionalization possibilities easier since polydopamine can be directly react with amine o thiol molecules. The polydopamine modification is a process bio-inspired by the mussel-chemistry. **Polydopamine coating is obtained by dopamine oxidative self-polymerization in a basic medium(pH=8.5**

SEM CHARACTERIZATION

Dopamine solution
2mg/mL
pH 8.5

Polydopamine film

RAMAN CHARACTERIZATION

The success in the polydopamine coating was corroborated by Raman spectroscopy, Figure

Polydopamine

Intensity

λ (cm⁻¹)

Figure 1. A) SEM Image of the top surface and the perpendicular section of the silicon nitride wafer; B, C and D) SEM Images considering the top surface and the perpendicular section of the silicon nitride wafer after the polydopamine polymerization. F) Raman spectrum of the silicon nitride surface after polydopamine modification.

WATER CONTACT ANGLE

84°

Polydopamine coating

60°

Figure 2. Water contact angles: Left) Silicon nitride surface and Right) silicon nitride coated with a polydopamine film.

AFM CHARACTERIZATION

329.5 nm

Mean square roughness of 23.6 nm

Figure 3. A and B) AFM images (2 and 3D) for the silicon nitride surface after poydopamine modification. Frame dimensions: 5μm × 5μm. C) Analysis of the roughness

CONCLUSIONS:

Poolished Silicon nitride surface can be easily modified with a thin film of polydopamine. The topography of surface was studied by SEM and AFM: The film consisted in a polydopamine cement with a large amount of aggregates of polydopamine nanoparticles dispersed along the surface.

After polydopamine modification: the silicon nitrides become more hydrophilic (60°) and more rough (mean square roughness of 23.6 nm).

Comments about posters, Joksa

A: Clean poster, minimal but effective use of colour, nanoparticles and nanorods, same information is given on both, easy to compare. One problem is that the bottom table lacks legend completely.

B: Good use of colour and the effort put in shows but this poster suffers from a terminal case of text overload, which makes the structure as a poster also difficult. Aims section helps to understand what the poster is about but after that there is just a lot of text.

C: The poster looks ok and is east to digest…but it is seriously lacking in content. Note that C scores quite OK in the visual clarity aspects, but it would get bad scores in the other parts of the matrix, especially content and depth.

D: This poster has too much content. For the amount of content, it is very well made. But the sheer amount of content makes it very difficult to understand what all is on the poster and how everything on it ties together

E: This poster lacks structure almost completely. What is where? Impossible to tell. It also has too many images for one poster.

F: This is a great poster. It has clear motivation explained in the oil-soaked bird, and then clearly titled sections where I can find what I want. I also subjectively like the colour choices (red and cyan as theme colours, matching to the bird and water?). The pictures and the text in them is of good size.

G: It looks a bit unfinished. On a good side, there is an OK number of results, but they do not seem to tell a clear story. This poster lacks text, it only has figures and captions, which might work but usually a bit of text is better than no text.

Topics:

1. Inertial microfluidics for circulating tumor cell screening
2. Acoustofluidics for circulating tumor cell screening
3. Droplet microfluidics for single cell RNA sequencing
4. Digital microfluidic immunoassays
5. Paper microfluidics: sensing opportunities beyond colorimetric detection
6. CD microfluidics based diagnostics: what are the advantages?
7. Liver-on-chip
8. Gut-on-chip
9. Human-on-chip: integrated organs on chip
10. Microchip capillary electrophoresis for environmental analysis
11. Multicellular organism on a chip (choose e.g. C.Elegans, zebrafish).

The poster and pair is selected in a Wiki in MyCourses.

We can now attempt to deal out as many topics as possible.

If you do not settle on a topic day, we try to do it through MyCourses before next weeks session.